This is a preprint, the final version is subject to change, of the American Mineralogist (MSA)
Cite as Authors (Year) Title. American Mineralogist, in press.
DOI: https://doi.org/10.2138/am-2020-7334

Revision 1

Effects of the dissolution of thermal barrier coating materials on the viscosity of remelted volcanic ash

Dirk Müller, Kai-Uwe Hess, Ulrich Kueppers, Donald B. Dingwell

Department for Earth and Environmental Sciences, Ludwig-Maximilians-Universität München, Theresienstrasse 41, 80333 Munich, Germany

Abstract

The chemical interaction between remelted volcanic ash and ceramic coatings of yttria-stabilized zirconia (YSZ) and / or gadolinium zirconate (GZO) is of special importance for the design of volcanic ash melt-resistant thermal barrier coatings (TBCs) for aviation turbine technologies. The spreading and infiltration potential of the melts is strongly influenced by the melt viscosity. Thus the interpretation of infiltration experiments and modeling of infiltration processes both rely on accurate viscosity data. Melt viscosity may be significantly altered by the dissolution of the YSZ or GZO thermal barrier coatings during the infiltration process. Here, we have determined the influence of YSZ and GZO additions to the viscosity of a series of volcanic ash melts using high temperature concentric cylinder viscometry. All samples have been characterized fully after viscometry. At 6.5 wt% of YSZ or GZO, both dopants lead to a reduction of viscosity in a temperature range between 1297-1640 °C in air. The magnitude of the decrease in viscosity depends weakly on volcanic ash melt composition. The viscosity effect has been parameterized in the following form:

$$\Delta\eta = x \cdot m_{dopant}$$

whereby x is a melt-composition specific coefficient of viscosity decrease, and m_{dopant} represents the added amount of YSZ / GZO (wt%). This viscosity reduction should contribute to an acceleration of the physical infiltration of TBCs via remelted volcanic ash.

Keywords: gas-turbine, aviation, rare earth oxides, yttria-stabilized zirconia (YSZ), gadolinium zirconate (GZO)

Introduction

Yttria-stabilized zirconia (YSZ) is a typical material used for thermal barrier coatings on turbine blades in aviation engines. Gadolinium zirconate (GZO) has been proposed as a potential replacement for YSZ in thermal barrier coatings in order to improve resistance to environmental dust. The lifetime of thermal barrier coatings (TBCs) is mainly limited by mechanical stresses, induced by thermal cycling, that lead to mechanical degradation and eventual exposure of the underlying alloy. Exposure of such TBCs to environmental debris in the atmosphere such as dust, sand or volcanic ash, initiates a further degradation of TBCs which is also chemical in nature as the ingested environmental debris may "remelt" (via melting of minerals or softening of a pre-existing glass phase) leading to chemical reaction with and partial dissolution of the TBC ceramics. Even in the absence of catastrophic failure of turbine engines due to TBC degradation, chronic exposure will lead to a substantial decrease in the lifetime of the TBCs and thereby increase operating costs substantially. YSZ (containing 6-8 wt% Y_2O_3) is state-of-the-art TBC material commonly used in the aviation industry (Clarke et al., 2012). It has however been demonstrated to possess a poor chemical resistance to attack by silicate melts at high temperatures (Zhao et al., 2014). Alternative TBC materials with higher chemical resistance to silicate melts are thus being investigated (Clarke

& Phillpot, 2005, Vaßen et al., 2010). Recently, gadolinium zirconate (GZO) has been shown to exhibit particularly improved performance in the presence of silicate melts (Krämer et al., 2008, Drexler et al., 2012).

The area as well as the infiltration depth and speed of silicate melts into TBCs is inferred to depend strongly on the viscosity of the melt (Jackson et al., 2015, Song et al., 2017) together with the TBC structure (Kabir et al., 2019) and chemical reactivity (Krämer et al., 2008, Drexler et al., 2012). Low viscosity melts are inferred to cover larger areas and infiltrate more easily into the open pore space of modern TBCs, leading to enhanced chemical reaction between the melt and the TBC and heightened risk of mechanical degradation during operative thermal cycling. The viscosity of silicate melts is strongly influenced by their chemical composition (Giordano et al., 2008). An enhanced concentration of network-formers (e.g. SiO_2) generally leads to more viscous melts, whereas network-modifiers (e.g., excess alkalis) generally act to decrease the viscosity.

It has been reported that the addition of Gd_2O_3 and / or Y_2O_3 to silicate melts will decrease the viscosity (Wang et al., 2012), while smaller amounts of up to 5 mol% ZrO_2 will increase viscosity (Barbieri et al., 2003, Karell et al., 2008). Recent viscosity models for multicomponent melts (Fluegel, 2007 and Giordano et al., 2008) do not incorporate Zr, Y or Gd and thus their influences on viscosity cannot yet be predicted for multicomponent melts. As a result, any model-based predictions represent a simplified estimate at best and an inaccurate one at worst in the resulting viscosity (Poerschke et al., 2016).

Here, we provide a direct experimental investigation of the effects of the addition of YSZ and GZO to five natural volcanic ash melts in an effort to alleviate this problem and to provide a parameterization suitable for modelling applications in volcanic ash melt TBC infiltration studies.

Materials & Methods

Materials Synthesis

Volcanic eruptions generate a wide range of volcanic ash whose bulk chemical compositions vary in silica content (40-75 wt%), alkali/aluminum ratio, iron content and oxidation state, and volatile contents. In an initial effort to span this wide range of compositions, we have chosen five ash samples of significantly different compositions: Krafla, Iceland (basalt) (Kr-L1); Tungurahua, Ecuador (andesite) (14TUN05); Cordon Caulle, Chile (rhyolite) (CoCa-1); Laacher See, Germany (phonolite) (LSB); Astroni, Italy (tephri-phonolite) (Astro-1). The Astroni and Tungurahua samples were naturally present in the form of volcanic ash (grain size < 2mm), whereas the other samples were composed of lapilli (2-64 mm). The lapilli samples were ground to an ash grain size using a tungsten carbide (WC) disk mill.

The volcanic ash samples were each doped by adding 6.5 wt% of yttria-stabilized zirconia (YSZ) powder (Y_2O_3/ZrO_2 8/92, 20-45 µm, GTV Verschleißschutz GmbH, Germany) or gadolinium zirconate (GZO) powder (Gd_2O_3/ZrO_2 60/40, 45-125 µm, Industriekeramik Hochrhein, Germany). Depending on the volcanic ash composition, the converted molar percent are 3.39-3.53 mol% YSZ and 1.70-1.77 mol% GZO (Supplementary material 1). Homogenization of the powder mixtures was performed by milling them in a WC disk mill.

Viscometry

Viscosity measurements were conducted at the Department for Earth and Environmental Sciences, LMU Munich. Powder mixes were melted into thin-walled Pt crucibles in air at 1500 °C for several hours in $MoSi_2$ resistance furnaces, then quenched by removal from the furnace to form glasses. Those glasses were extracted from the crucibles by pouring combined with drilling and/or percussion, depending on melt viscosity. The glasses were reloaded and remelted into viscometry measurement crucibles and then transferred to a viscometry furnace.

$Pt_{80}Rh_{20}$ spindles of standard dimensions were attached to a Brookfield viscometer head and then immersed in the samples and stirring commenced (Dingwell, 1986, Dingwell and Virgo, 1988). Measurement protocols started with the highest temperature measurements first and then a stepwise reduction of temperature (25 °C steps) until sample crystallization occurred or instrument limits were reached. At the end of each stepwise temperature decrease series the initial temperature and state was reoccupied to check for instrument drift or sample volatilization. The entire apparatus and set-up has been calibrated against standard glass DGG-1 (HVG-DGG). At the end of the reoccupation of the highest temperature data point the sample was removed from the furnace and allowed to cool to room temperature in air in the crucible. The sample was then subsequently drilled out of the crucible using diamond coring drills whose outer diameter was slightly less than the inner diameter of the crucible. These cored samples were then subjected to chemical and mineralogical analyses.

Electron probe microanalysis (EPMA)

The chemical compositions of the glass samples as well as crystals therein were determined using a Cameca SX-100 electron microprobe at the Department for Earth and Environmental Sciences, LMU Munich. In order to meet the requirements of the beam sensitive glass the following conditions were applied for glasses: 15 kV accelerating voltage, 5 nA sample current, and a 10 µm defocused beam. Crystalline phases were measured with a focused beam at 15 kV and 20 nA. Calibration was performed using the following silicate and oxide standards: albite (Na, Si), orthoclase (K, Al), hematite (Fe), periclase (Mg), wollastonite (Ca), ilmenite (Ti), bustamite (Mn), Cr_2O_3 (Cr), apatite (P), anhydrite (S), vanadinite (F), yttrium-iron garnet (YIG) (Y), gadolinium-iron garnet (GdIG) (Gd), zirconia (Zr), hafnium (Hf). Only results with totals between 98.5 – 101.5 wt% were accepted for evaluation.

X-ray fluorescence (XRF)

120 The original ash samples were ground for 5 minutes in a zirconia ball mill to obtain a fine-
121 grained powder. For XRF analyses, the samples were analyzed at the Institute of Geosciences,
122 Johannes Gutenberg University Mainz, Germany. Major elements were analyzed by
123 measuring fused glass beads (0.4 g sample, 5.2 g $Li_2B_4O_7$ flux) with a Philips Analytical
124 MagiX PRO.

125 Loss-on-ignition (LOI) was determined by weighing the sample before and after heat
126 treatment for 2 h at 980 °C.

127

128 **Results**

129 **Chemical composition**

130 The chemical compositions of the undoped samples were measured by EPMA and XRF (Fig.
131 1, Supplementary material 1). In order to crosscheck both analytical methods the results were
132 normalized to 100 % for comparison (excluding the LOI of XRF analyses). Those results are
133 in very good agreement (Supplementary material 1). Based on the TAS nomenclature (Le
134 Maitre et al., 2002) the samples can be assigned to basaltic (Krafla), andesitic (Tungurahua),
135 rhyolitic (Cordon Caulle), phonolitic (Laacher See) and tephri-phonolitic (Astroni)
136 compositions.

137 All GZO doped samples show homogeneous glasses, as proved by back-scattered electron
138 images and EPMA analyses (Supplementary material 1). Regarding the YSZ doped samples
139 only the Krafla and Tungurahua samples are entirely homogeneous, whereas very minor
140 amounts of Y-lean ZrO_2 spheres (rounded 50 micron particles) were found at the bottom of
141 the YSZ-doped Cordon Caulle, Laacher See and Astroni samples (Supplementary material 1).
142 Based on this study it is not possible to say whether these particles are undissolved, Y-leached
143 starting material (Xia et al., 2019) or are precipitates from the melt (Krämer et al., 2006) that

gravitationally settled at the bottom of the crucibles. The amounts of these crystals are insufficient to substantially influence the viscosity determinations or the bulk chemistry of the melts during measurements.

Viscometry

The viscosities of the undoped, low-alkali samples (Krafla, Tungurahua, Cordon Caulle) positively correlate with their SiO_2 content, while the alkali-rich, phonolitic samples (Laacher See, Astroni) show viscosities between the andesitic Tungurahua and the rhyolitic Cordon Caulle sample (Fig. 2, Supplementary material 2). It will be apparent at a first inspection that the addition of YSZ or GZO leads to a reduction of viscosity for all volcanic ash samples. To a first order, the magnitudes of viscosity reduction are also similar. In more detail, for the Krafla sample there is no observable difference between the viscosity reduction resulting from the additions of YSZ vs. GZO. The viscosity determinations for doped Krafla are also the most extensively documented as there was no evidence for oxidation or crystallization during the stepwise cooling. This is presumably due to a relatively high solubility of the YSZ and GZO dopants in this, the only low silica basaltic composition investigated in this study. For the Tungurahua and the Laacher See sample, the YSZ doping leads to a slightly stronger reduction of viscosity in comparison to the GZO dopant and *vice versa* for the Cordon Caulle and Astroni samples.

Amongst the YSZ-doped samples, only the YSZ Krafla sample viscosity was measured over the whole temperature range. For the Tungurahua, Cordon Caulle, Laacher See and Astroni samples, measurements were interrupted at temperatures where instabilities in the viscometry were observed which we tentatively assign to incipient high temperature crystallization. Degraded quality of viscometry signals led to their exclusion from further analysis.

168

169 ## Discussion

170 The overall reduction of viscosity in consequence of YSZ or GZO doping indicates that the
171 influence of the network-modifying agents Y_2O_3 and Gd_2O_3 dominates over any potential
172 network-forming capability of ZrO_2 in these melts. Based on the molar difference between the
173 YSZ and GZO dopant concentration (~3.5 mol% YSZ versus ~1.7 mol% GZO), that lead to
174 comparable viscosity reductions, it can be concluded that gadolinium has a stronger network-
175 modifying impact on silicate glasses than yttrium, consistent with the observations of Wang et
176 al. (2012). Since the variation of the molar fractions for YSZ and GZO within the different
177 volcanic ashes is very little (3.39-3.53 mol% YSZ and 1.70-1.77 mol% GZO), these
178 differences are regarded as negligible for the interpretation of the data. The dependency of
179 viscosity (η) reduction on the dopant amount is visualized in Fig. 3 and Fig. 4. Assuming a
180 linear relationship in first order, the following simplified parametrization can be done based
181 on viscosity values determined at 1590.6 °C:

182 $$\Delta\eta = x \cdot m_{dopant} \quad (1)$$

183 whereby x is a melt-composition specific coefficient of viscosity decrease (Tab. 1) and m_{dopant}
184 represents the added amount of YSZ / GZO (wt%). For parametrization, the theoretical
185 composition of 6.5 wt.% dopant concentration was used instead of taking the measured glass
186 composition after viscometry, as the latter ones might be influenced by high temperature
187 crystallization. The temperature of 1590.6 °C was chosen since it is the only temperature at
188 which viscosity data was measured for all samples (Supplementary material 2).

189

190 ## Implications

191 The high temperature viscosity data of five volcanic ash samples of basaltic, andesitic,
192 rhyolitic and phonolitic compositions, each doped with 6.5 wt% YSZ or GZO, reveal a
193 reduction of viscosity for all samples compared to their natural counterparts. With respect to
194 thermal barrier coatings it can be concluded, that once the dissolution of the YSZ or GZO
195 coating material in contact with a silicate melt starts, the viscosity will decrease, enabling an
196 enhanced spreading on the surface and / or infiltration in the coating. A simple
197 parameterization of the effects of YSZ and GZO on the viscosity of melts of volcanic ash
198 samples can be expressed as a linear relationship. This parameterization should be employed
199 in any future modelling of the dynamics of silicate (CMAS or natural ash) melt interaction
200 with TBCs.

201

202 **Acknowledgment**

203 We thank Hilger W. Lohringer for EPMA sample preparation. Gerhard Wolf is acknowledged
204 to make the YSZ and GZO powders available for us and Álvaro Amigo Ramos for collecting
205 the Cordon Caulle sample. DM acknowledges funding by the German Federal Ministry for
206 Economic Affairs and Energy (VAsCo, IGF No. 189 EN/2) and the support by the
207 LMUMentoring program as part of the German University Excellence Initiative. DBD
208 acknowledges the support of ERC Advanced Grant ADG-2018- 834225 (EAVESDROP).

209

210

211 **References**

212 Barbieri, L., Cannillo, V., Leonelli, C., Montorsi, M., Mustarelli, P., and Siligardi, C. (2003)
213 Experimental and MD Simulations Study of CaO-ZrO_2-SiO_2 Glasses, Journal of
214 Physical Chemistry B, 6519-6525.

Clarke, D.R., and Phillpot, S.R. (2005) Thermal barrier coating materials, Materials Today, 8, 22-29.

Clarke, D.R., Oechsner, M., Padture, N.P., and Guest Editors (2012) Thermal-barrier coatings for more efficient gas-turbine engines, MRS Bulletin, 37, 891-898.

Craig, M., Ndamka, N.L., Wellman, R.G., and Nicholls, J.R. (2015) CMAS degradation of EB-PVD TBCs: The effect of basicity, Surface & Coatings Technology, 270, 145-153.

Dingwell, D.B. (1986) Viscosity-temperature relationships in the system $Na_2Si_2O_5$-$Na_2Al_4O_5$, Geochimica et Cosmochimica Acta, 50, 1261-1265.

Dingwell, D.B., and Virgo, D. (1988) Viscosities of melts in the Na2O-FeO-Fe2O3-SiO2 system and factors controlling relative viscosities of fully polymerized silicate melts, Geochimica et Cosmochimica Acta, 52, 395-403.

Drexler, J.M., Chen, C.-H., Gledhill, A.D., Shinoda, K., Sampath, S., and Padture, N.P. (2012) Plasma sprayed gadolinium zirconate thermal barrier coatings that are resistant to damage by molten Ca-Mg-Al-silicate glass, Surface & Coatings Technology, 206, 3911-3916.

Fluegel, A. (2007) Glass viscosity calculation based on a global statistical modelling approach, Glass Technology: European Journal of Glass Science and Technology, Part A, 48, 13-30.

Giordano, D., Russell, J.K., and Dingwell, D.B. (2008) Viscosity of magmatic liquids: A model, Earth and Planetary Science Letters, 271, 123-134.

HVG-DGG (Hüttentechnische Vereinigung der Deutschen Glasindustrie e. V. - Deutsche Glastechnische Gesellschaft e.V.), http://www.hvg-

dgg.de/fileadmin/dateien/verein/Standardglas_Ia.pdf; http://www.hvg-dgg.de/fileadmin/dateien/verein/Standardglas_Ib.pdf

Jackson, R.W., Zaleski, E.M., Poerschke, D.L., Hazel, B.T., Begley, M.R., and Levi, C.G. (2015) Interaction of molten silicates with thermal barrier coatings under temperature gradients, Acta Materialia, 89, 396-407.

Kabir, M.R., Sirigiri, A.K., Naraparaju, R., and Schulz, U. (2019) Flow Kinetics of Molten Silicates through Thermal Barrier Coating: A numerical Study, Coatings, 9, 332.

Karell, R., Chromcikova, M., and Liska, M. (2008) Structure and properties of selected zirconia silicate glasses, Advanced Materials Research, 39-40, 173-176.

Krämer, S., Yang, J., and Levi, C.G. (2006) Thermochemical Interaction of Thermal Barrier Coatings with Molten CaO-MgO-Al2O3-SiO2 (CMAS) Deposits, Journal of the American Ceramic Society, 89, 3167-3175.

Krämer, S., Yang, J., Levi, C.G., and Johnson, C.A. (2008) Infiltration-Inhibiting Reaction of Gadolinium Zirconate Thermal Barrier Coatings with CMAS Melts, Journal of the American Ceramic Society, 91, 576-583.

Le Maitre, R. W., Streckeisen, A., Zanettin, B., Le Bas, M. J., Bonin, B., and Bateman, P. (Eds.) (2002) Igneous Rocks: A Classification and Glossary of Terms, Recommendations of the International Union of Geological Sciences Subcommission 30 on the Systematics of Igneous Rocks, Cambridge University Press, Cambridge, United Kingdom.

Poerschke, D.L., Barth, T.L., and Levi, C.G. (2016) Equilibrium relationships between thermal barrier oxides and silicate melts, Acta Materialia, 120, 302-314.

Rose, W.I., and Durant, A.J. (2009) Fine ash content of explosive eruptions, Journal of Volcanology and Geothermal Research, 186, 32–39.

Song, W., Lavallée, Y., Wadsworth, F.B., Hess, K.-U., and Dingwell, D.B. (2017) Wetting and Spreading of Molten Volcanic Ash in Jet Engines, The Journal of Physical Chemistry Letters, 8,1878-1884.

Vaßen, R., Jarligo, M.O., Steinke, T., Mack, D.E., and Stöver, D. (2010) Overview on advanced thermal barrier coatings, Surface & Coatings Technology, 205, 938-942.

Wang, M., Cheng, J., Li, M., He, F., and Deng, W. (2012) Viscosity and thermal expansion of soda-lime-silica glass doped with Gd_2O_3 and Y_2O_3, Solid State Sciences, 14, 1233-1237.

Xia, J., Yang, L., Wu, R.T., Zhou, Y.C., Zhang, L., Huo, K.L., and Gan, M. (2019) Degradation mechanisms of air plasma sprayed free-standing yttria-stabilized zirconia thermal barrier coatings exposed to volcanic ash, Applied Surface Science, 481, 860-871.

Zhao, H., Levi, C.G., and Wadley, H.N.G. (2014) Molten silicate interactions with thermal barrier coatings, Surface & Coatings Technology, 251, 74-86.

This is a preprint, the final version is subject to change, of the American Mineralogist (MSA)
Cite as Authors (Year) Title. American Mineralogist, in press.
DOI: https://doi.org/10.2138/am-2020-7334

276 **List of figure captions**

277 Fig. 1: Visualization of the chemical compositions of the used volcanic ashes, plotted in the
278 total alkali versus silica (TAS) diagram after Le Maitre et al. (2002).

279 Fig. 2: Results of the viscosity measurements for the undoped as well as the YSZ and GZO
280 doped volcanic ash samples. The error for viscosity is within the symbol size.

281 Fig. 3: Change in viscosity ($\Delta\eta$) in dependence of YSZ dopant amount at 1590.6 °C (left –
282 wt.%; right – mol%).

283 Fig. 4: Change in viscosity ($\Delta\eta$) in dependence of GZO dopant amount at 1590.6 °C (left –
284 wt.%; right – mol%).

285

286

287 Tab. 1: Melt composition dependent gradient (x) for calculation of viscosity decrease ($\Delta\eta$) through YSZ / GZO doping of

288 silicate melts (for wt.% and mol% values).

	YSZ (wt.%)	GZO (wt.%)	YSZ (mol%)	GZO (mol%)
Krafla	-0.0160	-0.0156	-0.0294	-0.0574
Tungurahua	-0.0321	-0.0249	-0.0609	-0.0941
Cordon Caulle	-0.0358	-0.0438	-0.0686	-0.1676
Laacher See	-0.0244	-0.0173	-0.0451	-0.0639
Astroni	-0.0275	-0.0385	-0.0507	-0.1414

289

290

This is a preprint, the final version is subject to change, of the American Mineralogist (MSA)
Cite as Authors (Year) Title. American Mineralogist, in press.
DOI: https://doi.org/10.2138/am-2020-7334

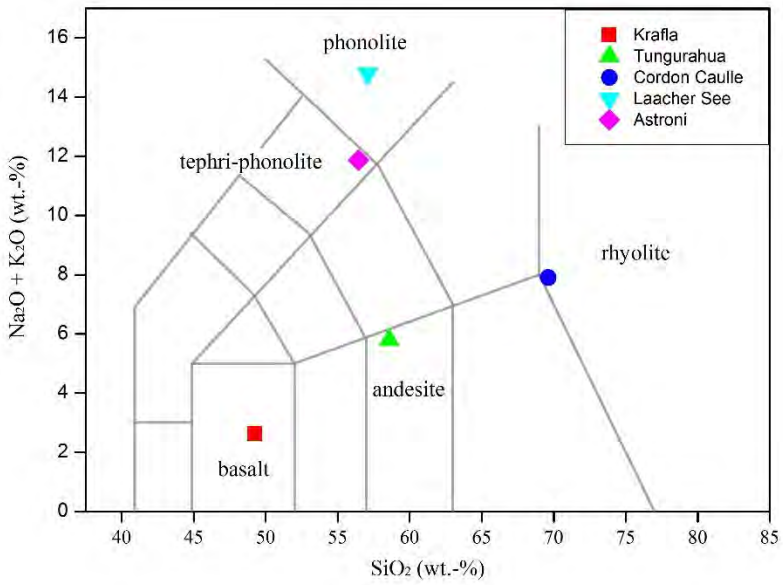

291

292 Figure 1: Visualization of the chemical compositions of the used volcanic ashes, plotted in the total alkali versus silica (TAS)

293 diagram after Le Maitre et al. (2002).

294

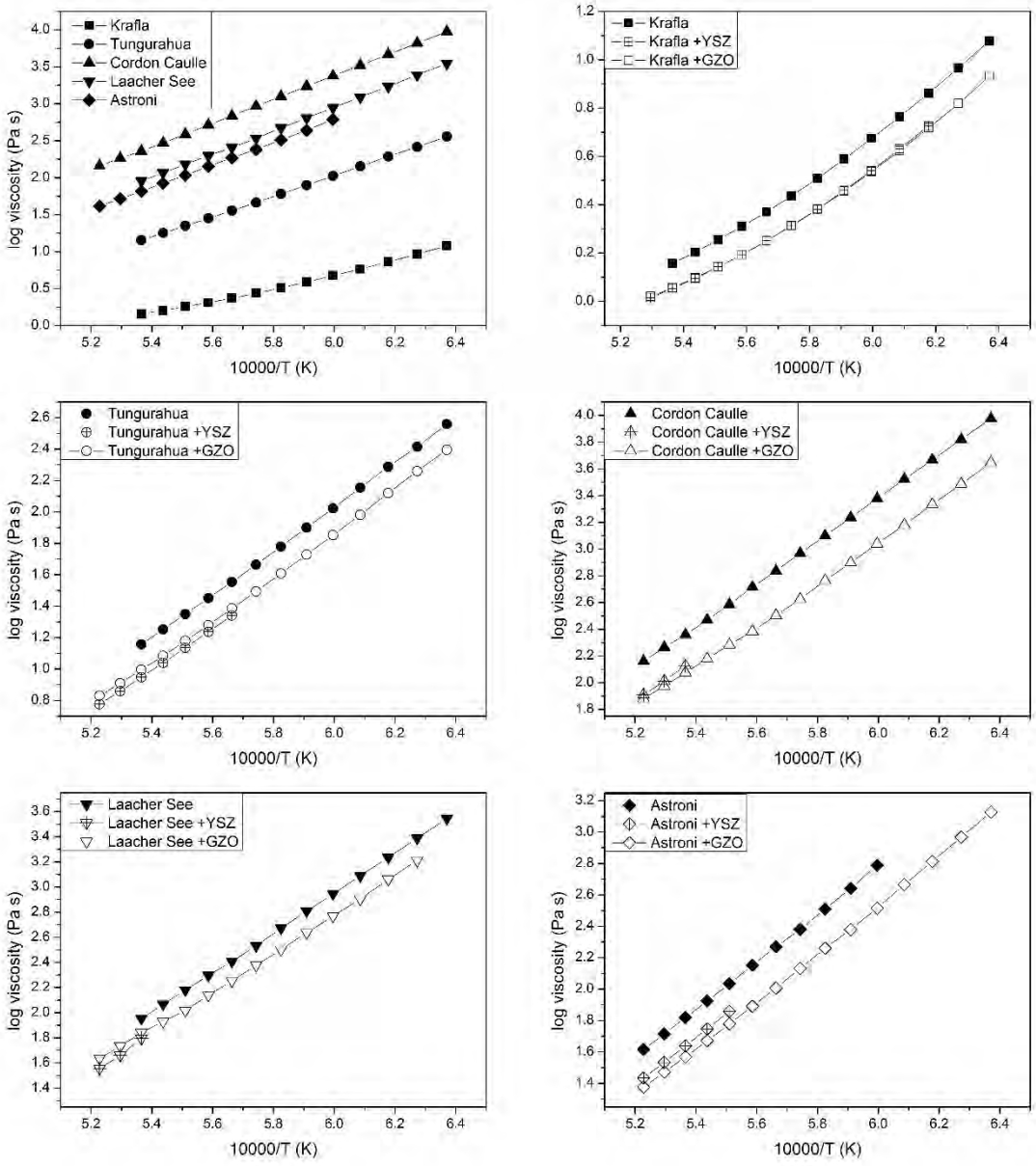

Figure 2: Results of the viscosity measurements for the undoped as well as the YSZ and GZO doped volcanic ash samples. The error for viscosity is within the symbol size.

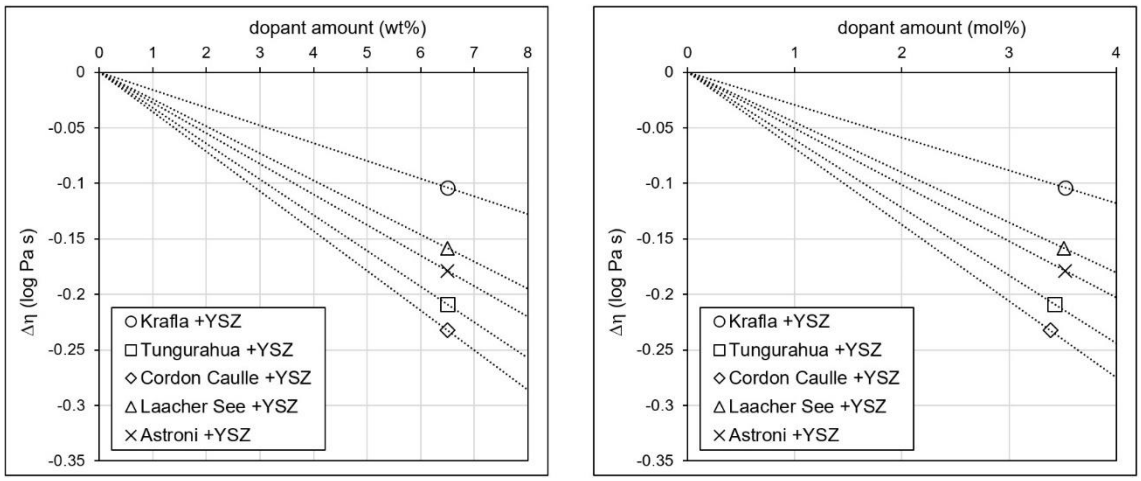

299

300 Figure 3: Change in viscosity (Δη) in dependence of YSZ dopant amount at 1590.6 °C (left – wt.%; right – mol%).

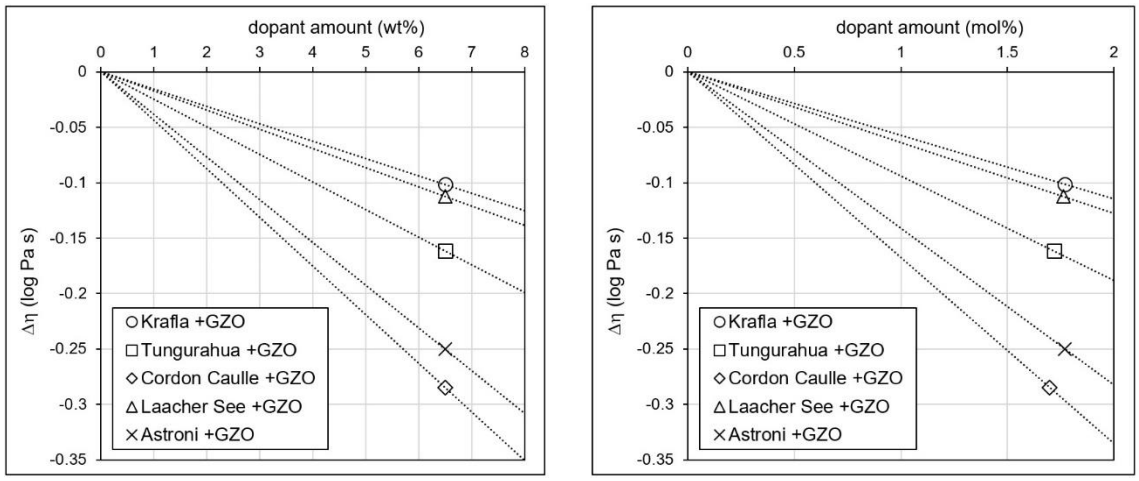

301

302 Figure 4: Change in viscosity (Δη) in dependence of GZO dopant amount at 1590.6 °C (left – wt.%; right – mol%).

303